Acta Mechanica XXX, 1–13 (2002) O/904

ACTA MECHANICA

Effect of nonuniform wall heating on the three-dimensional secondary instability of falling films

S. Miladinova, D. Staykova, Sofia, Bulgaria, **G. Lebon,** Liege, and
B. Scheid, Brussels, Belgium

(Received June 25, 2001)

Summary. Secondary three-dimensional instabilities of nearly sinusoidal waves on vertically falling and nonuniformly heated films are studied by using a long-wave evolution equation. Two-dimensional waves are unstable with respect to transverse modulations with sufficiently long spanwise wavelength. Two distinct three-dimensional modes of instability are examined: a synchronous mode which does not alter the wave number of the basic two-dimensional waves and a subharmonic mode with one-half of the streamwise wavenumber. According to a Floquet analysis, the subharmonic instability is most likely to be dominant for streamwise wavenumbers close to the neutral curve. The three-dimensional instability mechanism depends on film heating. The secondary growth rate increases (decreases) with increasing (decreasing) film heating downstream, but the contribution of thermocapillarity to synchronous and subharmonic instabilities is different.

1 Introduction

Fluid motion and heat transport in thin free surface liquid films are of fundamental interest in basic industrial equipment, as steam condensers, wetted wall columns, liquid film evaporators and other processes involving interfacial heat and mass transfer. In particular, the wavy free surface can enhance interfacial transfer. While the hydrodynamic behavior of thin wavy falling films has been studied extensively [1]–[7], only few studies [8]–[13] have shown that the presence of wall heating may have an important effect on the wave nature of falling films. Uniform as well as nonuniform heating of thin layers may cause considerable temperature differences at the interface, and thus thermocapillary force will draw liquid from the warmer region to the cooler one. This process will distort the original waveform.

Thin films moving over heated walls turn out to be unstable against long-wavelength infinitesimal perturbations, the same as in isothermal layers. Long-wavelength instability of thin liquid films flowing down an inclined nonuniformly heated plate was examined in earlier publications [11], [12]. The physical mechanism responsible for the stabilizing (destabilizing) effect of thermocapillarity in the case of a linear decrease (increase) in plate temperature downstream is explained. A nonlinear theory [13] shows the occurrence of finite-amplitude permanent waves that are monochromatic or broad-banded depending on the initial disturbance wavenumber at given Reynolds and Marangoni numbers. Several sudies [3]–[5] have demonstrated that two-dimensional interfacial waves on isothermal falling films are unstable with respect to both two- and three-dimensional disturbances and that the two-dimensional perma-

nent wave can become aperiodic by allowing transverse variations. Experimental observations [6], [7] confirm these theoretical predictions.

In the present study, we extend the two-dimensional study reported in [11] by considering a three-dimensional (3D) approach. The paper is organized as follows. In Sect. 2, we present the physical model of the non-isothermal film flow and we study the primary linear instability for the flat-film surface. The weakly nonlinear equilibration of primary instability into two-dimensional (2D) finite amplitude travelling waves is discussed. In Sect. 3, a linear three-dimensional analysis of secondary instability in the two-dimensional wave is developed. Two different transverse instabilities susceptible to deform the travelling waves are studied: a synchronous mode which does not alter the wave number of the basic 2D waves and a subharmonic mode with one-half of the streamwise wave number. In a concluding section, we summarize the results and discuss the 3D instability mechanism depending on the film thickness, wall heating and wave number of the primary 2D waves.

2 Physical model and primary instability

The three-dimensional film falling down a vertical non-uniformly heated plate is depicted in Fig. 1. The thin liquid layer is assumed to be Newtonian with density ϱ, kinematic viscosity ν and thermal diffusivity χ and is bounded to the right by a motionsless gas at ambient temperature T_g and pressure p_g. The free surface of the layer is considered as adiabatic. A constant temperature gradient A is imposed along the plate, and the plate temperature is $T_w = T_g + Ax$.

The flow rate is controlled mainly by changing the unperturbated film thickness d_0, which is used to define the Reynolds number $R = g{d_0}^3/\nu^2$, where g is the gravitational acceleration. The surface tension σ induces shear stresses as it depends on the temperature T and is given by

$$\sigma = \sigma_0 - \gamma(T - T_g)\,, \tag{1}$$

where σ_0 is the mean surface tension at temperature T_g and $\gamma = -d\sigma/dT$ is a positive constant for most common liquids. The mean surface tension is scaled by $S_0 = \sigma_0 d_0/\varrho\nu^2$.

We assume that the liquid film is very thin, so the ratio $\varepsilon = d_0/L$ is a small parameter, where $L \sim 2\pi/k_x$ is the characteristic streamwise length and k_x is the streamwise disturbance wave number. Here the x- and y-coordinates are scaled with L, z with d_0, time t with Ld_0/ν, and u and v are the velocity components in x and y-directions, respectively, scaled with ν/d_0. The temperature difference $T - T_g$ is scaled with the temperature difference $\left(T_w(L) - T_g\right) = AL$. The buoyancy effects are negligibly small for thin layers, and the intensity of heating affects the flow through thermocapillarity which is controlled by the Marangoni number, $Ma = \gamma AL d_0/\mu\chi = (\gamma A d_0/\mu\chi)\,\varepsilon^{-1} \sim O(\varepsilon^{-1})$. The Marangoni number is negative (positive) in the case of a linear decrease (increase) in plate temperature.

The wall heating influences the dynamics of liquid falling films through the shear-stress boundary conditions on the free surface, which at first-order approximation in ε are reduced to

$$u_z = -\frac{\varepsilon Ma}{P}\left(T_x + h_x T_z\right), \qquad v_z = -\frac{\varepsilon Ma}{P}\left(T_y + h_y T_z\right), \tag{2}$$

where the subscripts denote differentiation with respect to the indicated variable and $P = \nu/\chi$ is the Prandtl number.

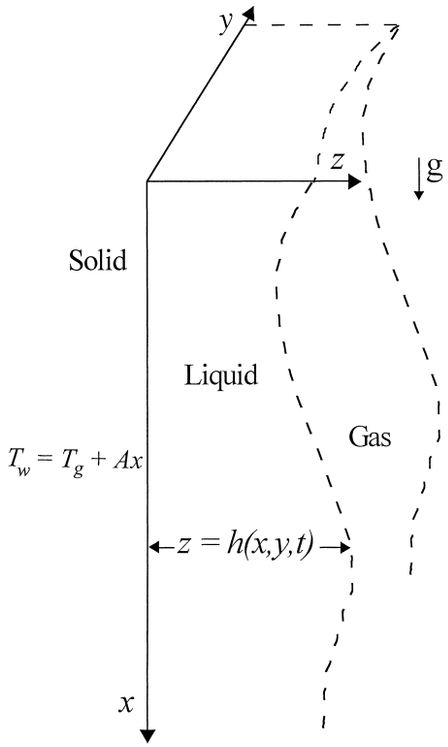

Fig. 1. Scheme of the film flow

We assume that the heat flux is moderate, and the induced gravity-driven flow is relatively slow, so that the flow regime is close to that predicted by the lubrication theory. For such kind of flows the long-wave approximation developed first by Benney [14] reduces the Navier-Stokes equations and boundary conditions to a single evolution equation for the local film thickness $h = h(x, y, t)$. The gravity, viscous, capillary and thermocapillary forces are assumed to be of the same order, thus R, P, $S = \varepsilon^2 S_0/3$ and $\varepsilon Ma \sim O(1)$. When the plate is heated non-uniformly, the long-wave evolution equation can be written as

$$h_t + (Rh - Mn)\, hh_x + \varepsilon\left[\frac{2}{15}\, Rh^5 h_x (Rh - Mn)\right]_x$$
$$+ \varepsilon\left\{\nabla.\left[\frac{PMn}{2}\, h^4 \left(\frac{5}{6}\, Rh - Mn\right)\nabla h\right] + \nabla.[S\, h^3 \nabla\nabla^2 h]\right\} + O(\varepsilon^2) = 0\,, \tag{3}$$

where ∇ is the surface gradient operator (∂_x, ∂_y) and $Mn = \varepsilon Ma/P$ is the rescaled Marangoni number. If one wishes to obtain a measure of the mean surface tension independently of the mean film thickness, one may replace S by the Kapitza number $Ka = R^{-1/3}S$. The second term in (3) describes the wave propagation, and the third and fourth terms represent the effects of nonlinear interaction of gravity and thermocapillarity. The local phase speed increases with the local film thickness and is influenced by thermocapillarity. Compared to the two-dimensional equivalent of (3) (see [11]), the fourth and the last capillary terms are different.

The basic state for the primary instability is a flat film, $h = 1$, with the velocity component in the x-direction given by $U(z) = Rz^2/2 - Mnz$ and zero velocities in y- and z-directions.

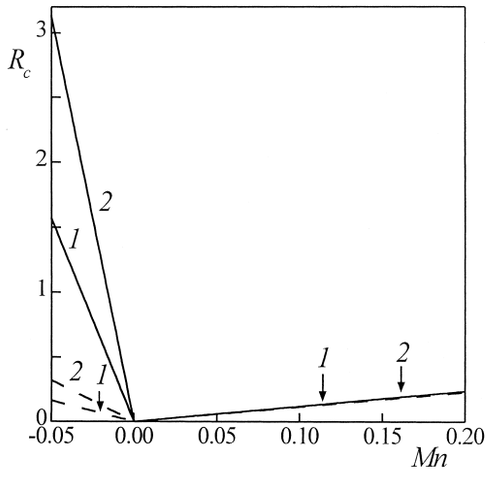

Fig. 2. Critical Reynolds number versus Mn for $P = 1$ (dashed line) and $P = 10$ (solid line): *1* - $\varphi = 0$ and *2* - $\varphi = \pi/4$

When the basic temperature is a linear function of the streamwise coordinate, Eq. (3) admits a normal-mode solution, $h(x, y, t) = 1 + \delta_0 \mathbf{e}^{(i\mathbf{k},\mathbf{x} - \omega_0 t)}$. Here $\delta_0 \ll 1$, $\mathbf{x} = (x, y)$, $\mathbf{k} = (k\cos\varphi, k\sin\varphi)$ is the wave number vector in the (x, y)-plane and $\omega_0 = \omega_r + i\omega_i$ is the complex frequency. The linearized phase speed of the perturbation is found to be $c_0 = \omega_i/k = R - Mn$, and the linear growth rate is given by

$$\omega_r = \left[\frac{2R}{15}\,(R - Mn)\,\cos^2\varphi + \frac{PMn}{2}\left(\frac{5}{6}\,R - Mn\right) - k^2 S\right]\varepsilon k^2\,. \tag{4}$$

In Fig. 2, the critical Reynolds number as a function of the Marangoni number is plotted for a two-dimensional wave ($\varphi = 0$) and an oblique wave ($\varphi = \pi/4$). The neutral curves for $P = 1$ are represented by the dashed lines for $P = 10$ by solid lines. The stable region exists for negative values of Mn due to the thermocapillary effect. This region disappears for $Mn = 0$, and there exists again a stable region for sufficiently intense heating. So, the primary instability is unconditional in the case of a weak linear increase in plate temperature. The value of the critical Reynolds number depends strongly upon P. It is seen that the influence of the Prandtl number on the three-dimensional threshold amplitude is related to the sign of the temperature gradient. Namely, when Mn is negative, R_c increases with P while for $Mn > 0$ it is independent of P.

A linear analysis of isothermal as well as uniformly heated layers predicts that the transverse variation is stabilizing in the primary instability but this is different in the secondary instability owing to the nonlinear interaction with the fundamental mode. Figure 2 confirms the validity of this conclusion for linear primary instability of non-uniformly heated layers when the initial instability is two-dimensional.

When the capillary force at the interface is taken into account, there exists a cut-off wavenumber, k_c, and the maximum growth rate occurs at $k_M = k_c/\sqrt{2}$. The cut-off wavenumber as a function of the Reynolds number for different values of the Marangoni number is plotted in Fig. 3. In the present work we choose physically reasonable values of the non-dimensional parameters. The Reynolds number is varied up to 5, the Marangoni number is estimated for a mean thickness $d_0 \approx 10^{-4}$ m, and $|A| \approx 1$ K/cm, $P = 10$ and $Ka = 4.2$ as in some experiments of Kabov et al. [15], and Scheid et al. [16] on films of 10% aequeous solutions of ethyl alcohol. The value k_c increases with R and decreases with Ka. As the Marangoni number increases to nonnegative values, the intersection between the upper neutral curve

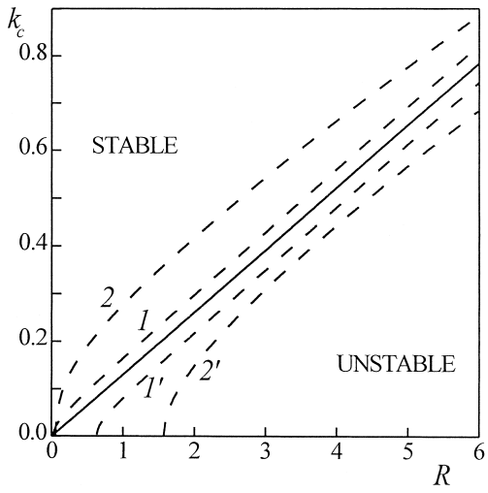

Fig. 3. Marginal stability wave number as a function of the Reynolds number, for $P = 10$, $Ka = 4.2$ and different values of the Marangoni number: --- *1* - $Mn = 0.02$, *2* - $Mn = 0.05$, *1′* - $Mn = -0.02$, *2′* - $Mn = -0.05$; the curve for $Mn = 0$ is represented by a continuous line

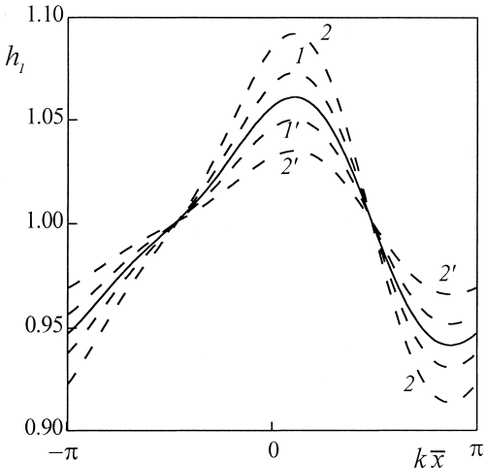

Fig. 4. Steady finite-amplitude wave h_1 of (5) at $R = 5$, $P = 10$ and $k = 0.8k_c$. The curve for $Mn = 0$ is represented by a continuous line; for $Mn \neq 0$ – by dashed lines: *1* - $Mn = 0.02$, *2* - $Mn = 0.05$, *1′* - $Mn = -0.02$, *2′* - $Mn = -0.05$

$k = k_c$ and the lower neutral curve $k = 0$ approaches the origin. Note that thermocapillarity can either increase or decrease the band of stable wavenumbers depending on the sign of Mn.

Nonlinear effects become important when the disturbance amplitude is small but finite. A weakly nonlinear analysis of non-uniformly heated films shows that the evolution of two-dimensional waves depends strongly on the initial disturbance wavenumber [11]. Moreover, there exists a value of k_s such that when $k_s < k < k_c$ the flow is supercritically stable, and nonlinear equilibration occurs after the initial instability. For $0 < k < k_s$, nonlinearity promotes the instability and the saturation does not occur. In the supercritical region, the free surface configuration, steady in the reference frame $\bar{x} = x - ct$, can be expressed as

$$h_1(\bar{x}) = 1 + 2[A_1 \cos(k\bar{x}) + A_2 \cos(2k\bar{x} + \theta)], \tag{5}$$

where the values of A_j $(j = 1, 2)$, c and θ are listed in [11]. The wave amplitude increases with decreasing k and vanishes at k_c, namely it bifurcates supercritically from k_c, and the lower bound of this supercritical instability is $k_s = k_c/2$. However, as k gets closer to k_s, higher harmonics become important and the equilibrated state cannot be represented by (5). The truncated series (5) describes well the free surface shape if $k_M < k < k_c$.

Typical forms of the steady finite-amplitude waves for various Marangoni numbers, when the other parameters are fixed, are plotted in Fig. 4 for $k = 0.8k_c$. In Fig. 3, the points $(5, 0.8k_c)$ are situated below the neutral curves and above the points $(5, k_M)$. The curves for $Mn \neq 0$ are represented by the dashed lines and for $Mn = 0$ by a solid line. Note, that the wave amplitude always grows as Mn increases, while the wave speed decreases weakly with Mn.

3 Secondary three-dimensional instability

Finite-amplitude 2D waves are generally unstable to $3D$ secondary instabilities. Patterns arising from two distinct 3D instabilities have been identified experimentally in [7]: synchronous transverse modulation and herringbone (or checkerboard) patterns. For the synchronous 3D pattern, the periodicity in the streamwise direction is the same as that of the primary 2D waves. The herringbone patterns are observed when the transverse phase of the modulations differs by π for successive wave fronts, and the streamwise period is doubled. The latter patterns are caused by a 3D subharmonic instability.

We will analyze the stability of 2D permanent waves to infinitesimal three-dimensional disturbances by using the Floquet theory of differential equations with periodic coefficients (e.g., [17]). The basic state h_1 for this secondary instability is given by (5). Equation (3) written in a frame moving with nonlinear speed c admits a normal mode solution with respect to y and t, and 3D disturbances can be written in the form

$$h_2(\bar{x}, y, t) = H(\bar{x})\, \mathbf{e}^{ily} \mathbf{e}^{\Gamma t}, \tag{6}$$

where $\Gamma = \Gamma_r + i\Gamma_i$ and the spanwise wavenumber l is assumed as real. The temporal growth rate of 3D disturbances is given by Γ_r, while Γ_i is a frequency shift with respect to the basic 2D wave frequency. When $h = h_1 + \delta h_2$, $\delta \ll 1$, is substituted into the evolution equation and the resulting equation is linearized in δ, an eigenvalue problem for $H(\bar{x})$ and Γ is displayed with

$$B_1 H''' + B_2 H''' + B_3 H'' + B_4 H' + (\Gamma + B_5)\, H = 0 \tag{7}$$

where a prime denotes differentiation with respect to $\bar{x}$ with coefficients B_j $(j = 1, \ldots, 5)$ which are given in the Appendix. The coefficients in (7) are periodic in $\bar{x}$, and the streamwise structure of the disturbances is given by

$$H = \mathbf{e}^{i\phi\bar{x}} \sum_{n=-\infty}^{\infty} a_n \mathbf{e}^{ikn\bar{x}}, \tag{8}$$

where ϕ is the Floquet exponent. Two cases for the Floquet exponent are distinguished: (*a*) $\phi = 0$, corresponding to synchronous solutions; (*b*) $|\phi| = k/2$, associated with subharmonic modes, i.e.,

$$\begin{aligned} H &= \sum_{n=\text{even}} a_n \mathbf{e}^{\frac{ikn\bar{x}}{2}}; \\ H &= \sum_{n=\text{odd}} a_n \mathbf{e}^{\frac{ikn\bar{x}}{2}} \end{aligned} \tag{9.1 - 2}$$

For synchronous modes, the series is truncated at $|n| \leq 4$, which includes a_{-4}, a_{-2}, a_0, a_2 and a_4, and for subharmonic modes at $|n| \leq 3$, which includes a_{-3}, a_{-1}, a_1 and a_3. We substitute

(9) in (7) to obtain an eigenvalue matrix problem and calculate the eigenvalues Γ for every value of the spanwise wave number l. We look for complex eigenvalues with the physical parameters fixed, and assign a value to the spanwise wave number. The eigenvalues are found using the routine DEVCCG from IMSL Library, and a performance index is computed to check the accuracy [18]. The performance of the eigensystem analysis routine is defined as excellent if the performance index is smaller than 1, and this is what is obtained in all of the cases we have considered. Stability results are presented for $\varepsilon = 0.1$, $P = 10$ and $Ka = 4.2$.

3.1 Synchronous instability

In this subsection we focus on synchronous solutions with wavelength $2\pi/k$. The eigenvalue with the largest real part is found to have $\Gamma_i = 0$, i.e. the fastest growing mode is purely real. This implies that one could have looked only for real eigenvalues. Typical curves for the linear growth rate are shown in Fig. 5 where Γ_r is plotted as a function of l. For $l = 0$ the eigenvalue is also zero. As l increases, Γ_r increases and remains positive, reaches a maximum Γ_{rM} at $l = l_M$, then decreases with increasing l and becomes zero at $l = l_c$. Thus, the two-dimensional waves are unstable for values of l between 0 and l_c, the upper boundary of the unstable wave numbers. In Fig. 5 we have considered four different cases of non-uniform heating with $R = 5$ and $k = 0.8k_c$. As a reference, the disturbance growth rate of the isothermal film $(Mn = 0)$ is also plotted. It is seen that Γ_{rM}, l_M and l_c increase with Mn. This means that the spanwise synchronous perturbations will grow (decay) when the temperature gradient along the plate is positive (negative). The basic state waveforms presented in Fig. 4 for different values of Mn show that the wave amplitude decreases as the parameter Mn becomes negative. So, the disturbance loses its energy when the thermocapillary force due to the upstream temperature gradiend is larger than the driving forces of the surface wave instability.

In Fig. 6, the Marangoni number is fixed to $Mn = -0.02$ (Fig. 6a) and $Mn = 0.02$ (Fig. 6b), and the streamwise wave number is varied. The important points of the curves are the maximum secondary growth rate Γ_{rM}, the corresponding value of the most amplified spanwise wavenumber l_M and the cut-off spanwise wave number l_c. The values of Γ_{rM} and l_M specify the expected observable secondary growth and the corresponding spanwise wave number. In the case $Mn = -0.02$ and $k = k_M$, the growth rate is substantially increased, the values of l_c and l_M are also larger. Near $l = 0$, the secondary growth rate of 2D waves with stream-

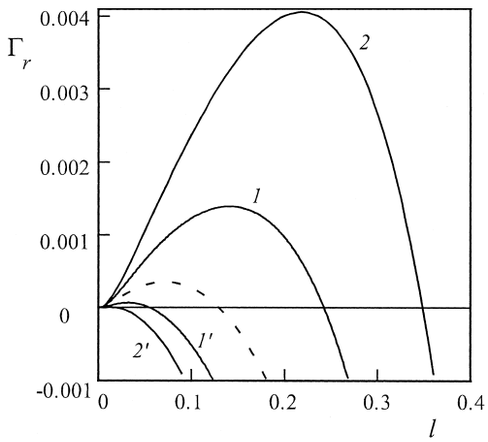

Fig. 5. Synchronous growth rate as a function of the spanwise wave number for $R = 5$ and different values of the Marangoni number: *1* - $Mn = 0.025$, *2* - $Mn = 0.05$, *1′* - $Mn = -0.025$, *2′* - $Mn = -0.05$; the curve for $Mn = 0$ is represented by a dashed line

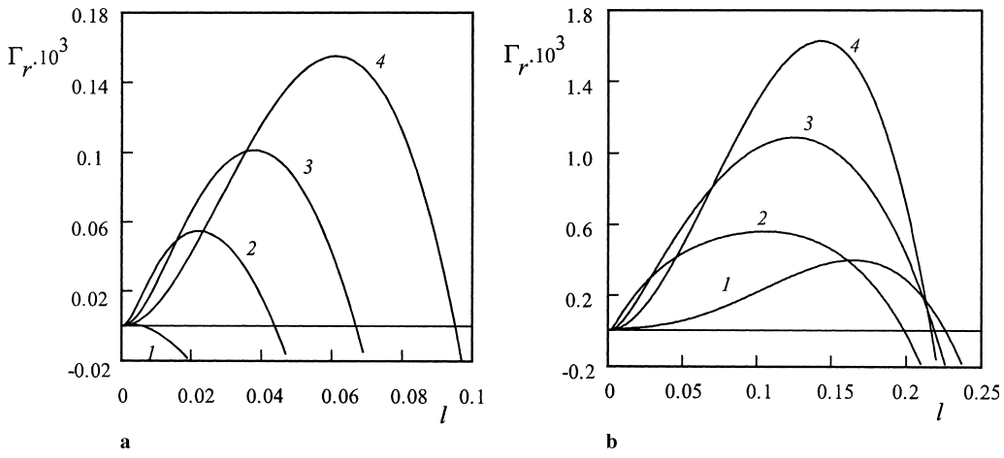

Fig. 6. Synchronous growth rate as a function of the spanwise wave number for $R = 5$ and different values of the streamwise wave number: *1* - $k = 0.99k_c$, *2* - $k = 0.9k_c$, *3* - $k = 0.8k_c$, *4* - $k = k_M$. **a** $Mn = -0.02$; **b** $Mn = -0.02$

wise wave number close to k_c is higher than that of respectively large amplitude waves. Comparison of the results for $Mn < 0$ and $Mn > 0$ shows that the behaviour of the secondary synchronous instability is not similar in both cases. In the case of a linear increase in plate temperature (Fig. 6b), near $k = k_c$ the maximum secondary growth rate as well as l_M decrease as k is decreased, and reach minima (at $k = 0.97k_c$), after which they increase. Joo and Davis [9] who studied the 3D instability of uniformly heated falling films suggested that the cut-off spanwise wavenumber should increase with decreasing k, the other parameters being fixed. Our instability analysis of nonuniformly heated films predicts that l_c oscillates slightly with k.

In order to examine the effect of thermocapillarity on the secondary synchronous instability, we plot Γ_{rM} in Fig. 7a, and l_c and l_M in Fig. 7b versus the Marangoni number at $k = 0.8k_c$. The curves are calculated for $R = 3$ (dashed lines) and $R = 5$ (solid lines).

The rate of increase of Γ_{rM} with Mn is very small for $Mn < 0$. Owing to the destabilizing thermocapillarity effect, for $Mn > 0$ the three-dimensional modes grow more rapidly than for $Mn < 0$. Liu et al. [7] examined 3D secondary instabilities of isothermal falling films for moderate R. They found experimentally that synchronous transverse modulations occur mainly along the troughs of the primary 2D waves. When $Mn > 0$ the thermocapillary force will draw the liquid from hot depressed regions to cooler elevated regions and the troughs will become warmer and shallower. This means that thermocapillarity will enhance significantly the synchronous mode of instability. In Fig. 7a, Γ_{rM} increases approximately ten times as Mn varies from 0 to 0.05. If the film heating decreases downstream, the temperature at the trough ahead of the moving wave front will be cooler than that at the peak. Hence, the thermocapillary force tends to flatten the free surface and to diminish the synchronous transverse modulations. As the mean layer thickness measured by R decreases, the driving force of the surface wave instability weakens and Γ_{rM} decreases at given Mn.

All values of l below the curves l_c are unstable, while values above the curves are stable (Fig. 7b). It is seen that the band of stable spanwise wave numbers decreases with Mn. For larger R ($R = 5$), the increase of l_c and l_M with Mn is almost linear. For smaller R ($R = 3$), the increase becomes strongly nonlinear, showing that the effect of thermocapillarity is more pronounced for very thin layers. For negative values of the Marangoni number the rate of

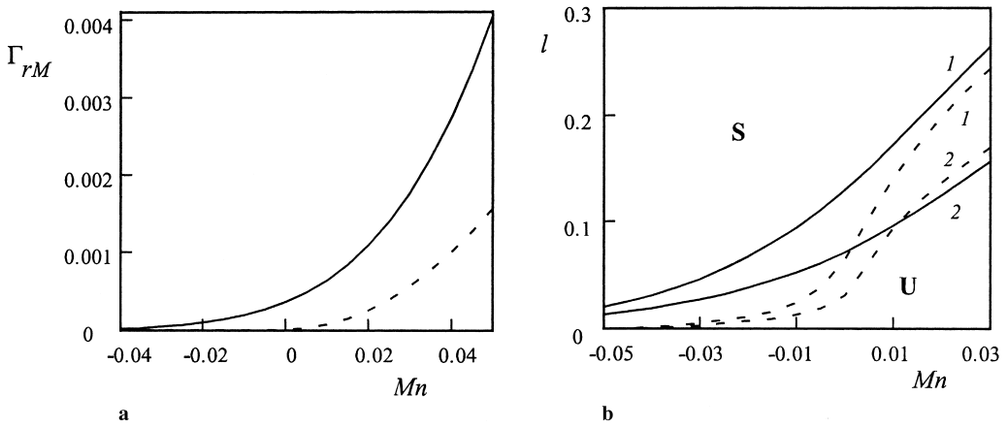

Fig. 7. The maximum growth rate of the synchronous 3D instability, the corresponding value of the most amplified spanwise wave number and the cut-off spanwise wave number as a function of the Marangoni number. Curves for $R = 5$ are represented by solid lines and these for $R = 3$ by dashed lines. **a** Γ_{rM}; **b** *1* - l_c, *2* - l_M, **S** - stable region, **U** - unstable region

increase of l_c and l_M with Mn at $R = 3$ is small, but as Mn becomes positive, the rate of increase becomes large. Calculated values of l_c and l_M are approximately independent on R when $Mn \geq 0.01$. Moreover, the most amplified spanwise wave number found at $R = 3$ is larger than that at $R = 5$. Our results at $Mn = 0$ agree qualitatively with measurements of Liu et al. [7] showing that l_M increases with increasing R. Recent experiments on films falling down a vertical, locally heated wall [15], however, suggest that the distance between crests in the spanwise direction increases weakly with the Reynolds number (i.e., l_M should decrease).

3.2 Subharmonic instability

The subharmonic eigenvalues Γ may become complex at low l but these complex transverse modes are always stable. So, the secondary modes travel synchronous with the modulated 2D waves. Synchronization provides an optimum chance for the transfer of energy into the three-dimensional disturbance. The variation of the growth rate for the subharmonic instability as a function of the spanwise wave number is shown in Fig. 8. There is a band of stable transverse wave numbers near zero. For $Mn < 0$ instability is restricted to a narrow band near $l = 0.2$ (curves $1'$ and $2'$), and this band broadens when the Marangoni number is increased. The range of maximum growth shifts toward larger values of l, and Γ_r increases with increasing Mn. The instability is sharply cut off at both a lower wave number l_{cL} and a higher wave number l_{cH}.

The important role of the streamwise wave number of the primary 2D wave is clearly shown in Fig. 9 where Γ_r is plotted versus l for different values of k. For values of k close to the neutral curve $k_c\ (R, Mn)$ the growth rate is sufficiently large. So, for k close to k_c, the two-dimensional travelling wave has a small amplitude, and the effect of 3D subharmonic instability is more pronounced. The growth characteristics for $Mn < 0$ (Fig. 9a) and $Mn > 0$ (Fig. 9b) vary with k in the same manner. In accordance with the results of Chang et al. [5] for isothermal films, our analysis predicts that the most amplified spanwise wave number decreases with increasing streamwise wave number; in contrast to that, Liu et al. [7] did not find a relation between k and l. The comparison of subharmonic and synchronous (see Fig. 6)

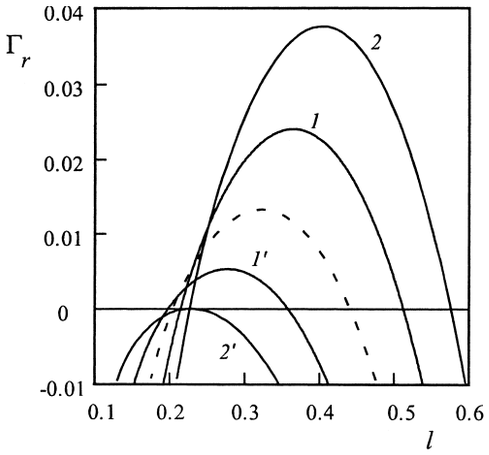

Fig. 8. Subharmonic growth rate as a function of the spanwise wave number for $R = 5$ and different values of the Marangoni number: *1* - $Mn = 0.02$, *2* - $Mn = 0.05$, *1′* - $Mn = -0.02$, *2′* - $Mn = -0.05$; the curve for $Mn = 0$ is represented by a dashed line

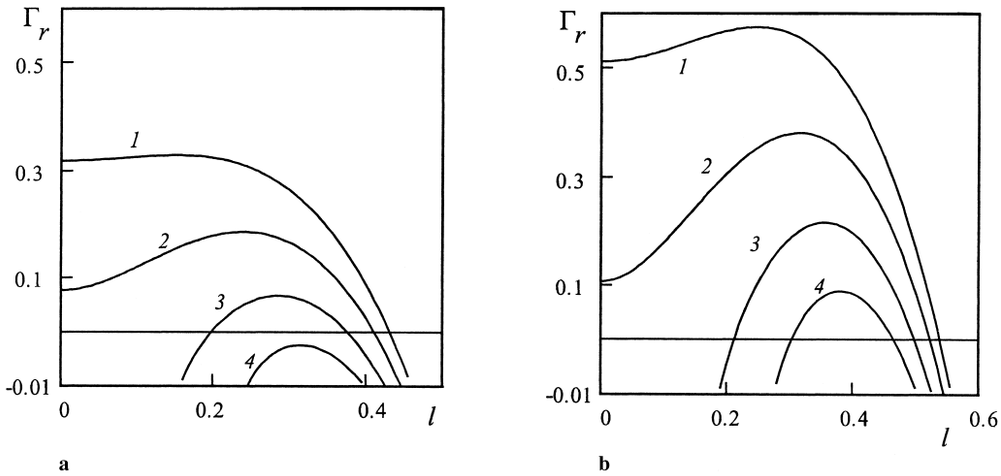

Fig. 9. Subharmonic growth rate as a function of the spanwise wave number for $R = 5$ and different values of the streamwise wave number: *1* - $k = 0.9k_c$, *2* - $k = 0.85k_c$, *3* - $k = 0.8k_c$, *4* - $k = 0.75k_c$. **a** $Mn = -0.02$; **b** $Mn = 0.02$

growth rates demonstrates that for nearly sinusoidal waves with small amplitudes the subharmonic 3D instability is dominant. This conclusion is in agreement with theoretical predictions presented in [5] and experimental observations in [7].

In Fig. 10, Γ_{rM}, l_{cL} l_M and l_{cH} are plotted versus Mn for the same values of the other parameters as in Fig. 7. The maximum growth rate (Fig. 10a) increases almost linearly as Mn is increased, with the Γ_{rM} being larger at large values of the Reynolds number. The rates of increase of Γ_{rM} with Mn for $Mn < 0$ and for $Mn > 0$ are similar. So, the contribution of thermocapillarity to the secondary growth rate of the subharmonic modes is quite different from that of the synchronous modes. The effect of thermocapillarity on the secondary 3D subharmonic instability is also seen in Fig. 10b. The growth rate is negative outside the region bounded by the l_{cL}- and l_{cH}-curves. There is a shift of this region to larger values of l when the Reynolds number is increased and the instability emanates from lower Marangoni number limit.

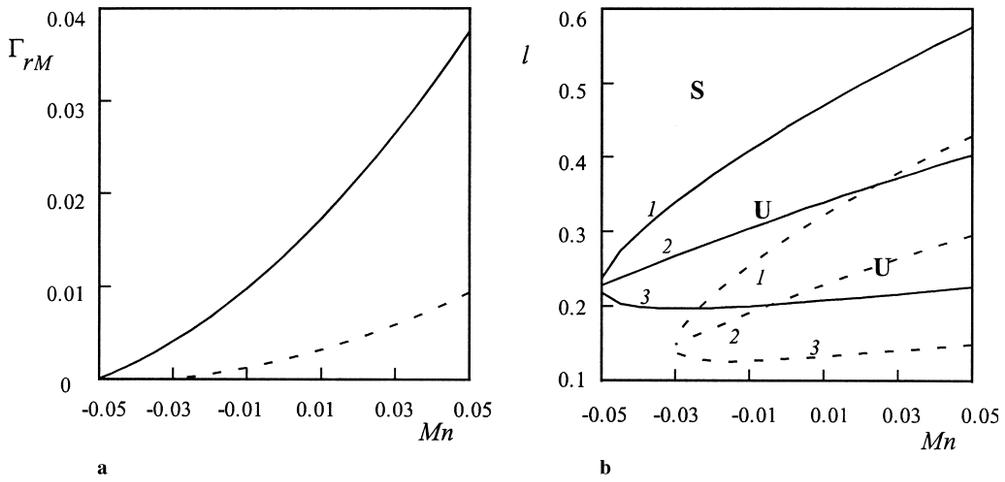

Fig. 10. The maximum growth rate of the synchronous 3D instability, the corresponding value of the most amplified spanwise wave number and the cut-off spanwise wave number as a function of the Marangoni number. Curves for $R = 5$ are represented by solid lines and these for $R = 3$ by dashed lines. **a** Γ_{rM}; **b** *1* - l_{cL}, *2* - l_M, *3* - l_{cH}, **S** - stable region, **U** - unstable region

4 Conclusions

The flow of a thin film falling down a vertical non-uniformly heated plate is investigated. The secondary transitions of the interfacial waves are studied via a long-wave evolution equation of Benney's type, with particular attention paid to the effect of thermocapillarity on the growth of secondary modes. The linear stability of finite-amplitude two-dimensional waves is analyzed using the Floquet theory. Two distinct instabilities are discussed in relation to the generation of 3D patterns observed in many experiments.

The small-amplitude waves are more susceptible to generate subharmonic 3D disturbances with long wavelength. When the streamwise wavenumber is close to the neutral curve, the maximum growth rate of the secondary subharmonic instability is comparable with that of the primary instability. According to Floquet's analysis, synchronous instability is likely to occur at lower wavenumbers, since its growth rate becomes comparable with the subharmonic growth rate for $k < k_M$. However, when the streamwise wavenumber is very small, the primary wave profiles are far from sinusoidal [13], and weakly nonlinear theories cannot be used. Extensive numerical calculations of the strongly nonlinear Eq. (3) are required to obtain the range of parameters over which the synchronous instability will occur.

The variation of the subharmonic growth rate with the Marangoni number is quite different from that of the synchronous growth rate. The influence of thermocapillarity on the 3D synchronous instability is related to the sign of the temperature gradient. When the film heating decreases downstream, the thermocapillary effect weakens and the fastest growing synchronous mode increases with the Reynolds number. In the case of a linear increase in the plate temperature, the 3D synchronous instability depends strongly on the Marangoni number and the effect of a small variation in mean film thickness is less pronounced.

In experimental studies [15]–[20], a constant flux was imposed on a rectangle area of the wall, with the horizontal sides of the rectangle quite longer than the vertical ones, to ensure conditions for forming two-dimensional flows. Indeed, at small flow rates and heat fluxes, almost two-dimensional structures are observed in the middle region of the heated area. In

particular, a stationary bump of the free surface appears closely to the upper side of the rectangle. The reason for such strong surface deformation is attributed to the thermocapillary force acting in the opposite direction to gravity. Direct measurement of the surface temperature confirm this suggestion because the temperature first increases significantly reaching a maximum and then decreases monotonically in the downstream direction. Above some moderate values of the heat flux (depending on the Reynolds number), regular three-dimensional patterns are also observed. There exist several vertical "horse-shoe"-like structures the number of which depends on the magnitude of the heat flux through the wall, especially the number of these structures decreases with increasing the heat flux. So far, there is not a proper theoretical model that describes these features of the film flow on a locally heated wall. It is worth noting that the distribution of the free surface temperature can be represented locally by a linear function of the longitudinal coordinate, especially when the temperature decays monotonically. Our theoretical predictions show that for 3D instabilities the expected observable spanwise wave number decreases when the plate temperature decays monotonically. New experiments with longer test sections are required to check the validity of our theory.

Appendix

Coefficients of Eq. (7)

$$B_1 = \varepsilon S {h_1}^3 ,$$

$$B_2 = \varepsilon 3 S {h_1}^2 {h_1}' ,$$

$$B_3 = \varepsilon {h_1}^2 \left[\frac{2R^2}{15} {h_1}^3 + \frac{5R}{12} Mn {h_1}^2 \left(P - \frac{8}{25} \right) - \frac{P}{2} Mn^2 h_1 - 2l^2 S \right] ,$$

$$B_4 = (Rh_1 - Mn) h_1 - c + \varepsilon {h_1}^2 {h_1}' \left(\frac{8R^2}{5} {h_1}^3 + \frac{25}{6} RMn \left(P - \frac{8}{25} \right) {h_1}^2 - 4PMn^2 h_1 - 3l^2 S \right) ,$$

$$\begin{aligned} B_5 = {} & (2Rh_1 - Mn) {h_1}' + \varepsilon {h_1}^2 {h_1}'' \left(\frac{4R^2}{5} {h_1}^3 + \frac{25}{12} RMn \left(P - \frac{8}{25} \right) {h_1}^2 - 2PMn^2 h_1 \right) \\ & + \varepsilon h_1 ({h_1}')^2 \left[\left(4R^2 {h_1}^3 + \frac{25}{3} RMn \left(P - \frac{8}{25} \right) {h_1}^2 - 6PMn^2 h_1 \right) + 3S (h_1 h_1''')' \right] \\ & + \varepsilon {h_1}^3 l^2 \left(-\frac{5}{12} RMnP {h_1}^2 + \frac{P}{2} Mn^2 h_1 + Sl^2 \right) . \end{aligned}$$

Acknowledgements

This work was partially supported by the European Community Contracts IC15-CT98-0908 and ICOPAC HRPN-CT2000-00136 and by the Interuniversity Pole of Attraction (IUAP convention IV 06) initiated by the Belgian State, Science Policy Programming.

References

[1] Chang, H.-C.: Wave evolution on a falling film. Ann. Rev. Fluid Mech. **26,** 103 – 136 (1994).
[2] Alekseenko, S. V., Nakoryakov, V. Ye., Pokusaev, B. G.: Wave flow of liquid films. New York: Begell House 1994.

[3] Joo, S. W., Davis, S. H.: Instabilities of three-dimensional viscous falling films. J. Fluid Mech. **242,** 529 – 547 (1992).
[4] Joo, S. W., Davis, S. H.: Irregular waves on viscous falling films. Chem. Eng. Comm. **118,** 111 – 123 (1992).
[5] Chang, H.-C., Demekhin, E. A., Kopelevich, D. I.: Nonlinear evolution of waves on a vertically falling film. J. Fluid Mech. **250,** 433 – 480 (1993).
[6] Liu, J., Paul, J. D., Gollub, J. P.: Measurements of the primary instabilities of film flows. J. Fluid Mech. **250,** 69 – 101 (1993).
[7] Liu, J., Schneider, J. B., Gollub, J. P.: Three dimensional instabilities of film flows. Phys. Fluids **A7,** 55 – ■ ■ (1995).
[8] Joo, S. W., Davis, S. H., Bankoff, S. G.: Long-wave instabilities of heated falling films: two-dimensional theory of uniform layers. J. Fluid Mech. **230,** 117 – 146 (1991).
[9] Joo, S. W., Davis, S. H., Bankoff, S. G.: A mechanism for rivulet formation in heated falling films. J. Fluid Mech. **321,** 279 – 298 (1996).
[10] Oron, A., Davis, S. H., Bankoff, S. G.: Long-scale evolution of thin liquid films. Rev. Modern Phys. **69,** 931 – 980 (1997).
[11] Slavtchev, S., Miladinova, S., Lebon, G., Legros, J.-C.: Marangoni effect on the instability of non-uniformly heated falling liquid films. In: Proc. 1st Intern. Symp. on Microgravity Research & Appl. in Phys. Sciences & Biotechnology, Sorrento, September 2000, (SP-454), **1,** 33 – 41 (2001).
[12] Kalitzova-Kurteva, P., Slavtchev, S., Kurtev, I.: Linear instability in liquid layers on an inclined, non-uniformly heated wall. Theor. Appl. Mech. **30,** 12 – 23 (2000).
[13] Miladinova, S., Slavtchev, S., Lebon, G., Legros, J.-C.: Long wave instabilities of non-uniformly heated falling films. (Submitted).
[14] Benney, D. J.: Long waves on liquid films. J. Maths. Phys. **45,** 150 – 155 (1966).
[15] Kabov, O. A., Marchuk, I. V., Chupin, V. M.: Thermal imaging study of the liquid film flowing on a vertical surface with local heat source. Russ. J. Eng. Thermophys. **6,** 104 – 138 (1996).
[16] Scheid, B., Kabov, O., Minetti, C., Colinet, P., Legros, J.-C.: Measurement of free surface deformation by reflectance-Schlieren method. In: Proc 3rd European Thermal-Science Conf., Heidelberg, **2,** 651 – 657 (2000).
[17] Herbert, Th.: Secondary instability of boundary layers. Ann. Rev. Fluid Mech. **20,** 487 – 526 (1988).
[18] Smith, B. T.: Matrix eigensystem routines: Eispack Guide, Springer 1976.
[19] Kabov, O. A.: Formation of regular structures in a falling liquid film upon local heating. Thermophysics and Aeromechanics **5,** 547 – 551 (1998).
[20] Kabov, O. A., Marchuk, I. V., Muzykantov, A. V., Legros, J.-C., Istasse, E., Dewandel, J. L.: Regular structures in locally heated falling liquid films. In: Proc. 2nd Int. Symp. on Two-Phase Flow Modelling and Experimentation (Celata, G. P., Di Marco, P., Shah, R. K., eds.), Pisa, **5,** 1225 – 1233 (1999).

Authors' addresses: S. Miladinova and D. Staykova, Institute of Mechanics, Bulgarian Academy of Sciences, Acad. G. Bonchev Street 4, 1113 Sofia, Bulgaria, (E-mail: svetla@imbm.bas.bg); G. Lebon, Institute of Physics, University of Liege, B-4000 Liege; B. Scheid, Microgravity Research Center, Universite Libre de Bruxelles, B-1050 Brussels, Belgium